Supplemental Materials

A. EQUATIONS

A.1. *Equivalent Width*

The *equivalent width* (or W_λ) is a measure of the area subtended by a spectral line, defined as

$$W_\lambda = \int_{\lambda_-}^{\lambda_+} \left(1 - \frac{I_\lambda}{I_c}\right) d\lambda \tag{A.1}$$

This parameter is related to the column density of absorbers (in this case CO in the lower state of the 3-2 R 14 transition) by the *curve of growth.* In the absence of a robust model for this curve, we choose to use W_λ as a qualitative measure of the CO column density, as it is an integral quantity and therefore more robust to spectral noise than the line core intensity.

A.2. *Epoch Analysis Model*

To model the growth and decay of the "cold bubbles" in the epoch analysis, we chose an exponential model where we treat the growth and decay timescales independently:

$$W_{tot}(t) = W_0 + A \times \begin{cases} 2^{(t-t_0)/\tau_+} & t < t_0 \\ 2^{-(t-t_0)/\tau_-} & t > t_0 \end{cases} \tag{A.2}$$

Here, W_0 is the steady-state "background" equivalent width (0 in the normalized epoch model), A is the bubble amplitude (normalized to unity), t_0 is the time where the bubble peaks (shifted to 0) and $\tau_\pm$ are the growth and decay rates, respectively. This model was chosen based on the apparent self-similarity of the individual equivalent width curves, and justified by theoretical discussions of autocatalytic CO cooling in the solar atmosphere.

A.3. *Timescale Analysis*

By interpreting the values of $\tau_\pm$ that are returned from the epoch analysis in terms of autocatalytic molecular cooling, we can estimate the height of the "bubbles" in the solar atmosphere by equating $\tau_\pm$ to a theoretical chemical evolution timescale:

$$t_{CO}^{chem} \approx 0.5 \left(\frac{T}{5000\,\mathrm{K}}\right)^{-16.2} \left(\frac{n_H}{1 \times 10^{15}\,\mathrm{cm}^{-3}}\right)^{-1} \ \mathrm{sec} \tag{A.3}$$

Using a temperature of 4000 K (obtained from the brightness temperature of the CO line core in the bubble, compared to the quiet-Sun average CO temperature of 4200 K), we can convert any measured value of $\tau_\pm$ into a gas density n_H. Those densities can then be associated with a height in a particular solar model, such as the average-Sun FAL-C model.

B. SUPPLEMENTAL FIGURES

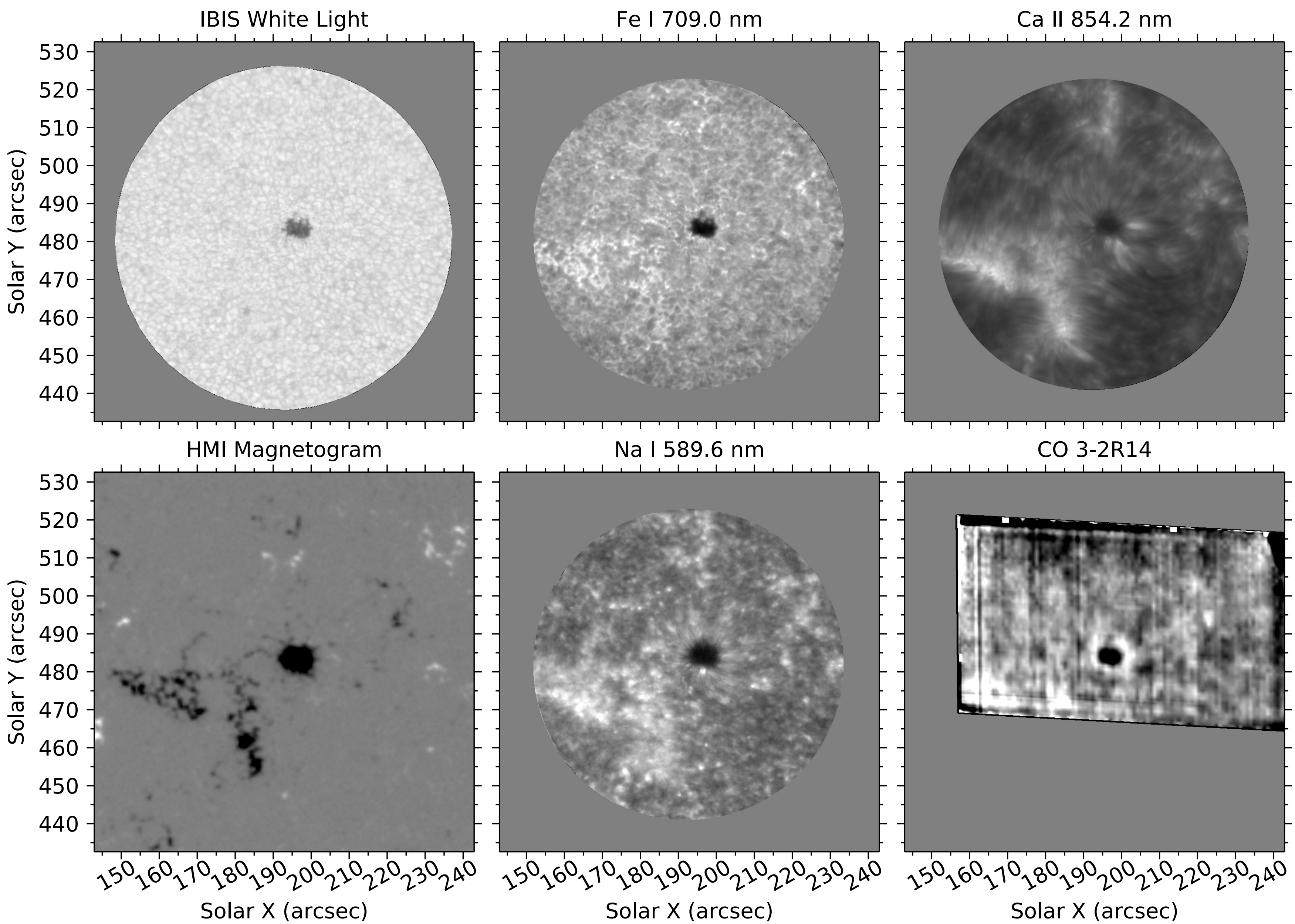

Figure B.1. Comparison of the line core intensities in the four observed spectral diagnostics. The left two panels show the IBIS white light reference (*top*) and HMI magnetogram (*bottom*). The line core intensities are shown for the photospheric Fe I and Na I lines (middle panels), and for the chromospheric Ca II line and the CO 3-2 R 14 line (right panels), the latter of which forms in the temperature minimum. The IBIS scan shown here was captured between 17:35:46 UTC and 17:36:06 UTC, while the CO scan was captured between 17:34:54 UTC and 17:35:49 UTC. To the lower right of the pore, one of the "cold bubbles" (a long-lived CO absorption event) can be seen. See the Github repository for a movie of the full observing sequence.

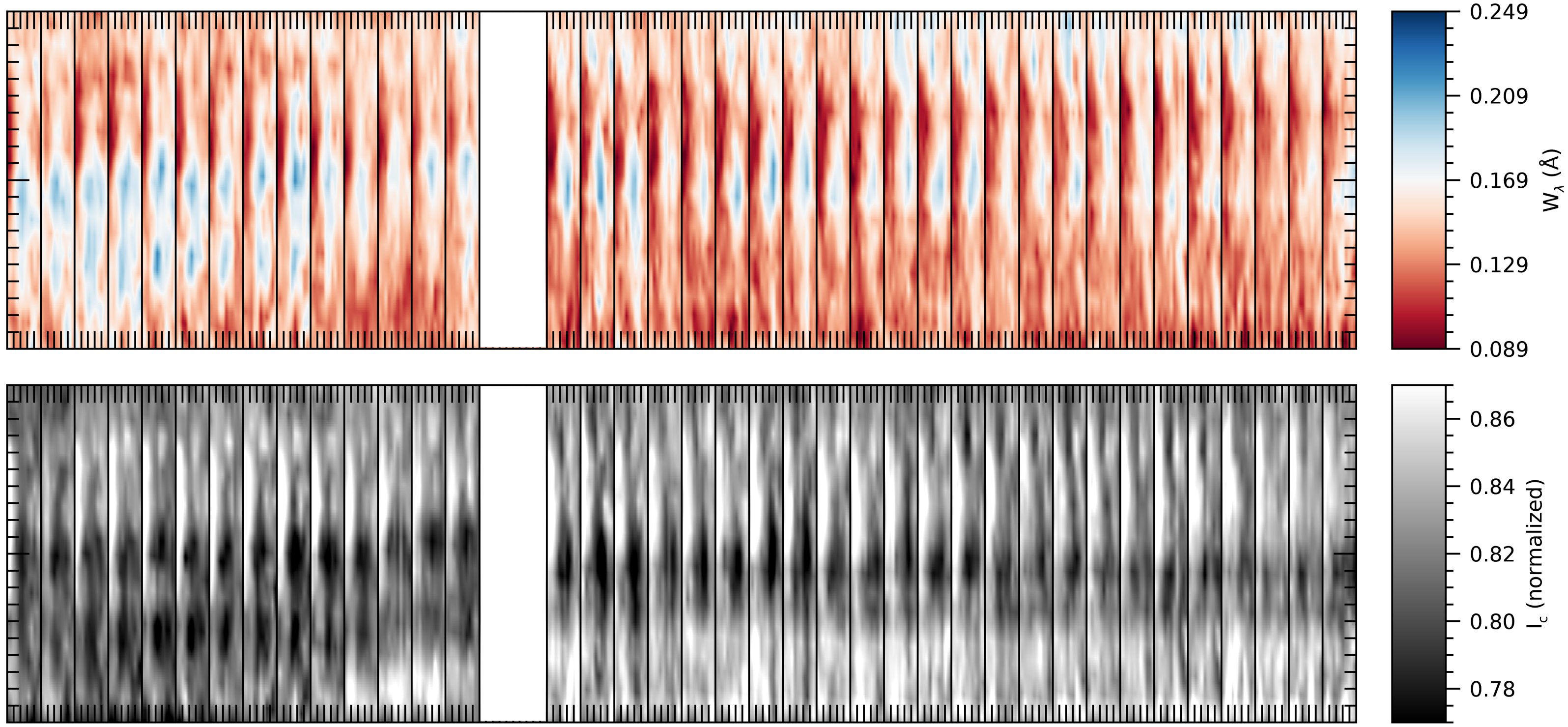

Figure B.2. A space-time diagram showing both the equivalent width (top) and the line core intensity (bottom) of the "cold bubble" seen in Figure B.1. The ticks on the x-axis represent 2" intervals, while the ticks on the y-axis represent 1" intervals. The white bar corresponds to two scans where the telescope was significantly off-pointed, such that no co-aligned data could be recovered. Each time step of 58 s is outlined in black and the overall temporal interval covered is ~ 39 minutes. The "bubble" comprises a region of unusually low brightness temperature and high equivalent width (i.e. CO density).

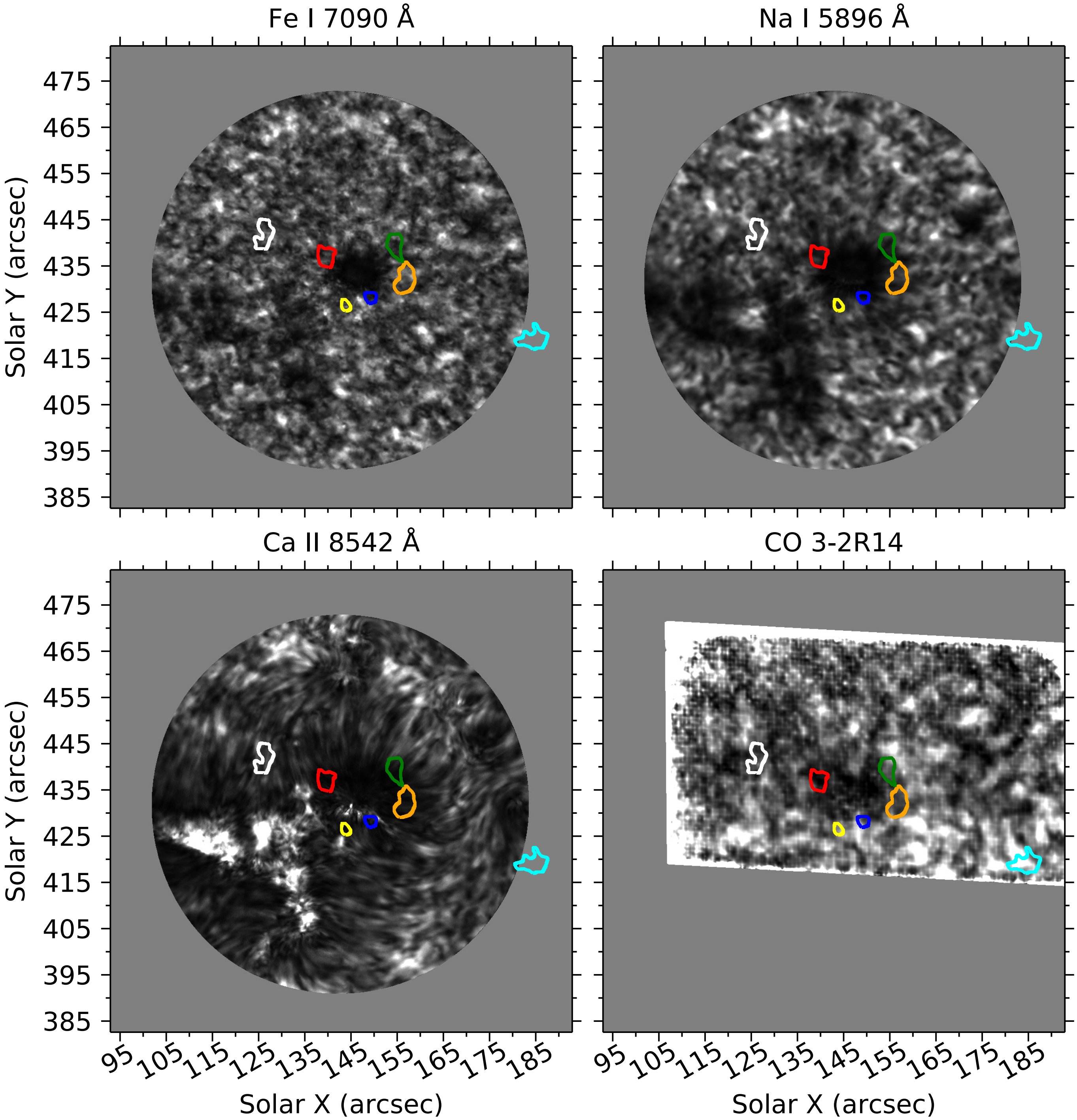

Figure B.3. Maps of the 5-minute (3.5 mHz − 5.5 mHz;top row) power in the Doppler velocity of each spectral line. The 5-minute band corresponds to the dominant helioseismic oscillations in the photosphere. The colored contours show the locations of the eight "cold bubbles".

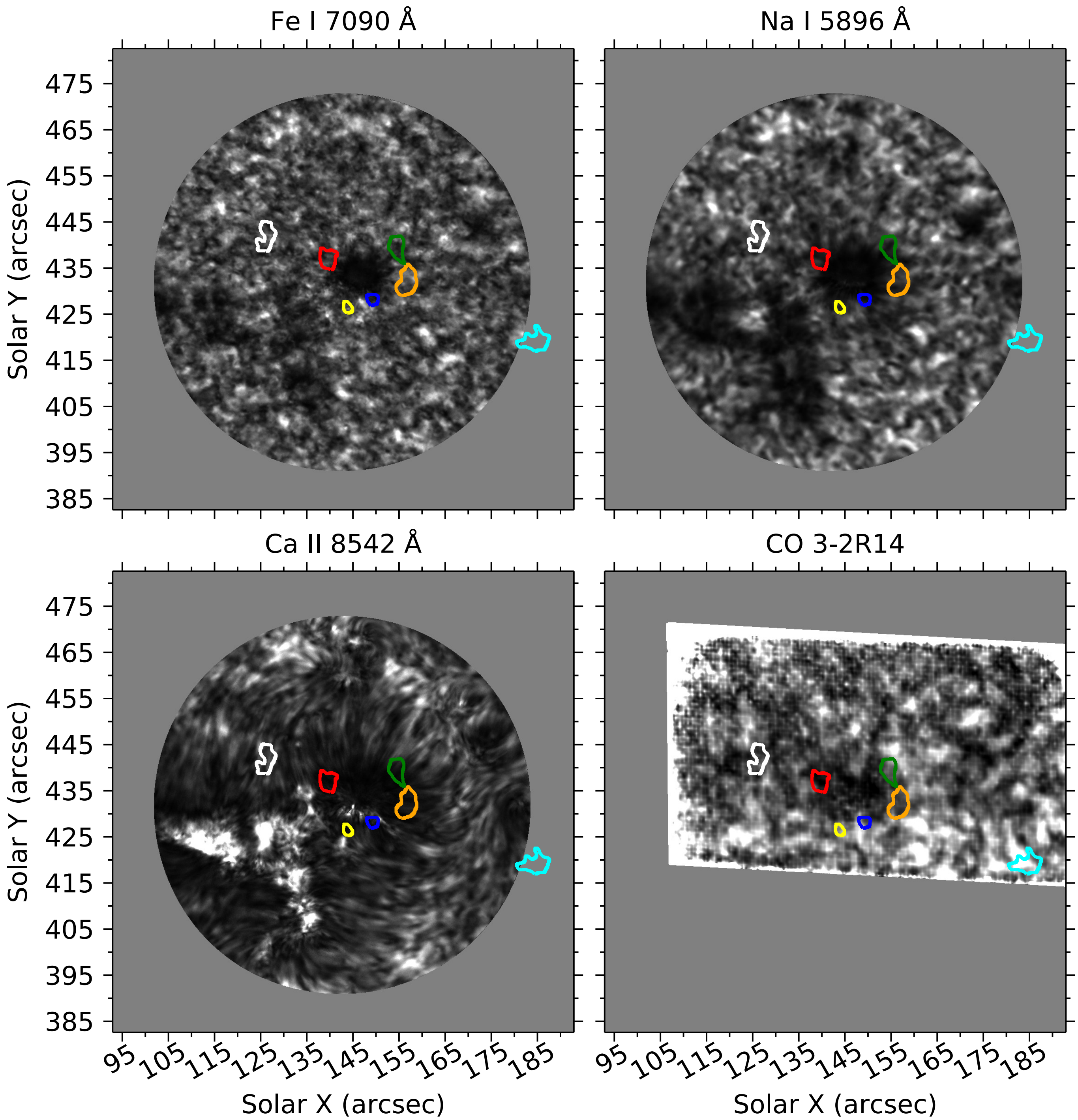

Figure B.4. Maps of the 3-minute (5.7 mHz − 7.7 mHz; bottom row) power in the Doppler velocity of each spectral line. The 3-minute band measures the power in frequencies just above the acoustic cutoff $\omega_c \approx 5.5$ mHz. The colored contours show the locations of the eight "cold bubbles". Note that the 3-minute power is depressed surrounding the pore in all four lines (also shown in Figure B.5), a phenomenon referred to as its "magnetic shadow".

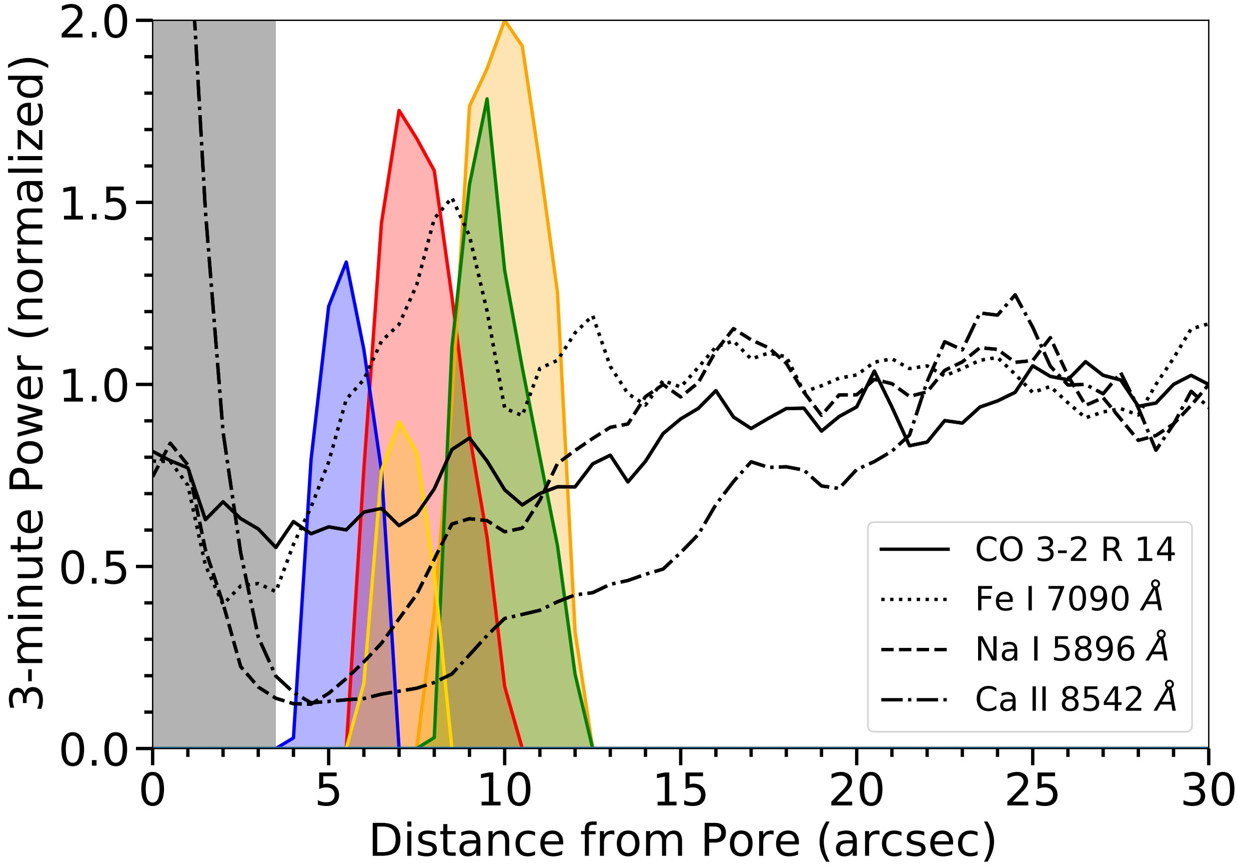

Figure B.5. The radially averaged 3-minute power surrounding the pore observed in CO (black), Fe I 7090 Å (red), Na I 5896 Å (blue), and Ca II 8542 Å (orange). All four curves have been normalized to the average quiet-Sun power. The grey shaded region represents the extent of the pore, while the colored shaded regions show the locations of the five bubbles surrounding the pore (color coded to match Figure 1 on the poster). Taller/wider peaks correspond to larger "bubbles". Note that the "bubbles" all lie within the magnetic shadow of the pore.

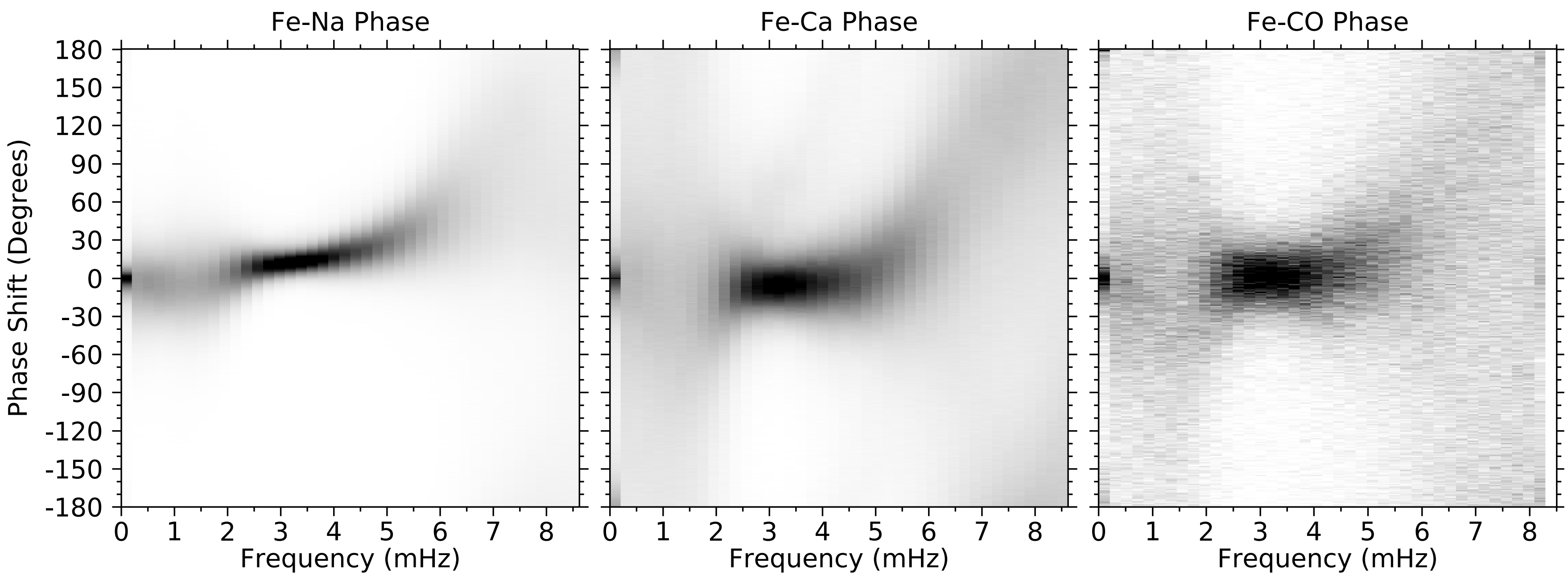

Figure B.6. Doppler velocity phase spectra of Na I 5896 Å (left) Ca II 8542 Å (center), and CO 3-2 R 14 (right) with respect to Fe I 7090 Å. Each column represents a histogram of observed phase shifts between Fe I and the listed line for oscillations in a given Fourier frequency bin. Note the slight curvature in the CO phase spectrum above the acoustic cutoff ($\sim 5\,\mathrm{mHz}$), compared to Figure 4 on the poster (which is flat). This implies that CO 3-2 R 14 forms higher than Fe I 7090, as expected.